Syntheses and Characterization of Novel Three-Dimensional Tellurites, $Na_2MTe_4O_{12}$ (M = W, Mo), with Intersecting Tunnels

Vidyavathy Balraj and K. Vidyasagar*

Department of Chemistry, Indian Institute of Technology, Madras, Chennai 600 036, India

Received May 18, 1999

Two isostructural tellurium-rich tellurites, $Na_2WTe_4O_{12}$ (**1**) and $Na_2MoTe_4O_{12}$ (**2**), have been synthesized and structurally characterized by single-crystal X-ray diffraction studies. Three types of polyhedra, namely, MO_6 octahedra, TeO_3 pyramids, and TeO_5 square-pyramids, constitute the three-dimensional $(MTe_4O_{12})^{2-}$ (M = W, Mo) anionic framework, which contains different types of intersecting tunnels, one of them being novel spiral pseudohexagonal tunnels occupied by sodium ions. Both compounds have the monoclinic space group *C*2/*c*, with $Z = 4$. The lattice parameters are as follows: for **1**, $a = 17.348(3)$ Å, $b = 5.7755(10)$ Å, $c = 11.269(3)$ Å, $\beta = 104.33(2)°$; for **2**, $a = 17.341(4)$ Å, $b = 5.8262(11)$ Å, $c = 11.268(2)$ Å, $\beta = 104.38(2)°$. Syntheses and structure, powder X-ray diffraction, and infrared spectroscopic studies of these compounds are described.

Introduction

We have undertaken an exploratory synthetic investigation of A−M−Te−O quarternary "phase space" for crystalline tellurite compounds, as there are only a limited number of ternary tellurites with extended structures. Moreover, tellurium in the +4 oxidation state is known to exist in a variety of coordinations, pyramidal TeO_3, TeO_4 with SF_4 geometry, and TeO_5 square pyramids, which could lead to a rich structural chemistry. Tellurites in the amorphous state, on the other hand, have been widely investigated[1−4] and are believed to contain tellurium in one or more of the possible coordinations. It is noteworthy in this context that tellurite glasses are studied from the point of view of developing new devices such as optical shutters[3] or switches and new laser systems because some of them exhibit high nonlinear optical susceptibility and upconversion-pumped fluorescence.[4] To understand and evaluate the likelihood of the structures in tellurite glasses, Becker et al. have reported[5] the crystal structures of the potassium tellurites $K_2Te_2O_5$ and $K_2Te_4O_9$, in which tellurium is found in both pyramidal TeO_3 and TeO_4 units with SF_4 geometry.

We have isolated, by a variety of synthetic methods, including hydrothermal techniques, a number of novel low-dimensional tellurites of molybdenum, namely, hexagonal tungsten oxide related, layered $A_2Mo_3TeO_{12}$ (A = NH_4, Cs) phases, "zero-dimensional" $A_4Mo_6Te_2O_{24}\cdot H_2O$ (A = Rb, K) compounds,[6] one-dimensional $A_4Mo_6TeO_{22}\cdot 2H_2O$ (A = NH_4, Rb) compounds,[7] and a two-dimensional $(NH_4)_6Mo_8Te_8O_{43}\cdot H_2O$ phase[8] containing discrete anions in another anion with an extended framework. Interestingly, the layered tellurites are noncentrosymmetric and exhibit a nonzero second-harmonic generation response. During our hydrothermal synthetic attempts to prepare layered and zero-dimensional tellurites of tungsten containing sodium, we have isolated a tellurium-rich tellurite compound, $Na_2WTe_4O_{12}$, possessing a three-dimensional anionic $(WTe_4O_{12})^{2-}$ framework with different types of intersecting tunnels, one of them being a novel spiral hexagonal tunnel occupied by Na^+ ions. Further, Te^{4+} is found to be present as both pyramidal TeO_3 and square-pyramidal TeO_5. Here, we report the syntheses and characterization of $Na_2WTe_4O_{12}$ (**1**) and its isostructural molybdenum analogue, $Na_2MoTe_4O_{12}$ (**2**).

Experimental Section

Synthesis. $Na_2WO_4\cdot 2H_2O$, $Na_2MoO_4\cdot 2H_2O$, and TeO_2 of high purity were used for both hydrothermal and ceramic syntheses. Teflon-lined, 23-mL-capacity acid digestion bombs from Parr were employed for hydrothermal synthesis.

$Na_2WTe_4O_{12}$ (1). A 0.707 g (2.143 mmol) sample of $Na_2WO_4\cdot 2H_2O$ and 0.114 g (0.714 mmol) of TeO_2 (Na:W:Te = 6:3:1) and 4.2 mL of water were heated in an acid digestion bomb at 225 °C for 4 days and then cooled to room temperature over a period of 36 h. $Na_2WTe_4O_{12}$ was obtained as the only product (0.158 g, 96% yield) in the form of a pale yellow powder and small amounts of tiny crystals. These tiny crystals were hand-picked and found to be suitable for single-crystal X-ray diffraction studies.

$Na_2MoTe_4O_{12}$ (2). A mixture of $Na_2MoO_4\cdot 2H_2O$ (0.726 g, 3.0 mmol) and TeO_2 (0.160 g, 1.002 mmol) in a 6:3:1 Na:Mo:Te ratio was heated along with 4.2 mL of water under the same hydrothermal conditions employed for compound **1**. Shiny, yellow crystals of $Na_2MoTe_4O_{12}$ were obtained as the only phase (0.207 g, 98% yield).

Polycrystalline samples of compounds **1** and **2** were prepared also by solid state reactions, by heating stoichiometric mixtures of appropriate chemicals in open air, initially at 450 °C for 6 h and then at final temperatures of 580 and 625 °C, respectively, for 2.5 days with three intermittent grindings.

X-ray Diffraction and Crystal Structure. The powder X-ray diffraction patterns were recorded on a Rigaku Miniflex (Table model) instrument using Co Kα radiation ($\lambda = 1.7902$ Å) and also on a Seifert automated powder diffractometer using Cu $K\alpha_1$ radiation (a Germanium single crystal was used as a monochromator; Cu $K\alpha_1$, $\lambda = 1.5406$ Å).

(1) (a) Tatsumisago, M.; Minami, T.; Kowada, Y.; Adachi, H. *Phys. Chem. Glasses.* **1994**, *35*, 89. (b) Tatsumisago, M.; Lee, S.-K.; Minami, T.; Kowada, Y. *J. Non-Cryst. Solids* **1994**, *177*, 154. (c) Himei, Y.; Osaka, A.; Nanba, T.; Miura, Y. *J. Non-Cryst. Solids* **1994**, *177*, 164.
(2) (a) Dimitriev, Y.; Dimitrov, V.; Arnaudov, M. *J. Mater. Sci.* **1979**, *14*, 723. (b) Dimitriev, Y.; Dimitrov, V.; Arnaudov, M. *J. Mater. Sci.* **1983**, *18*, 1353. (c) Dimitrov, V. *J. Solid State Chem.* **1987**, *66*, 256.
(3) Nasu, H.; Matsushita, O.; Kamiya, K.; Kobayashi, H.; Kubodera, K. *J. Non-Cryst. Solids* **1990**, *124*, 275.
(4) Tanabe, S.; Hirao, K.; Soga, N. *J. Non-Cryst. Solids* **1990**, *122*, 79.
(5) Becker, C. R.; Tagg, S. L.; Huffman, J. C.; Zwanziger, J. W. *Inorg. Chem.* **1997**, *36*, 5559.
(6) Vidyavathy, B.; Vidyasagar, K. *Inorg. Chem.* **1998**, *37*, 4674.
(7) Vidyavathy, B.; Vidyasagar, K. *Inorg. Chem.* **1999**, *38*, 1394.
(8) Vidyavathy, B.; Vidyasagar, K. *Inorg. Chem.* **1999**, *38*, 3458.

10.1021/ic990547i CCC: $18.00
Published on Web 11/23/1999

Table 1. X-ray Powder Diffraction Patterns of $Na_2WTe_4O_{12}$ (**1**) and $Na_2MoTe_4O_{12}$ (**2**)

			$Na_2WTe_4O_{12}$			$Na_2MoTe_4O_{12}$		
h	*k*	*l*	d_{cal}[a] (Å)	d_{obs} (Å)	I/I_0	d_{cal}[b] (Å)	d_{obs} (Å)	I/I_0
2	0	0	8.395	8.400	18			
1	1	0	5.453	5.458	30	5.506	5.500	28
1	1	−1				5.085	5.077	19
4	0	0				4.197	4.194	29
3	1	−1	4.007	4.010	100	4.030	4.028	77
3	1	−2	3.549	3.552	25	3.566	3.563	12
1	1	−3	3.144	3.143	49	3.152	3.155	18
3	1	2	2.990	2.998	30			
4	0	2	2.988					
5	1	−1	2.966	2.966	72	2.976	2.976	49
1	1	3	2.919	2.919	25			
0	2	0	2.883	2.885	48	2.914	2.911	100
6	0	0				2.798	2.798	15
0	0	4				2.723	2.720	11
2	2	−1				2.722		
2	2	1	2.597	2.597	59	2.618	2.618	29
4	0	−4	2.600					
4	2	0				2.394	2.393	16
7	1	−1				2.279	2.279	16
0	2	3	2.259	2.257	16			
6	0	−4	2.251					
4	2	2	2.075	2.074	27	2.084	2.085	29
4	2	−4				1.940	1.941	10
6	2	−3	1.907	1.907	18			
8	0	−4	1.907					
1	3	1				1.891	1.891	16
1	3	−2				1.836	1.836	14
9	1	−2	1.819	1.817	18			
0	0	6	1.818					
3	3	−2	1.768	1.768	25	1.782	1.784	23

[a] $a = 17.328(61)$ Å, $b = 5.765(23)$ Å, $c = 11.257(43)$ Å, $\beta = 104.34(16)°$. [b] $a = 17.339(39)$ Å, $b = 5.827(14)$ Å, $c = 11.248(27)$ Å, $\beta = 104.52(13)°$.

Silicon was used as an external standard. The indexed powder X-ray diffraction patterns of compounds **1** and **2** are given in Table 1. The observed powder X-ray diffraction patterns agree well with those simulated on the basis of their single-crystal structural data using the LAZY-PULVERIX program,[9] indicating the monophasic nature of the compounds.

Single crystals of compounds **1** and **2**, suitable for X-ray diffraction studies, were mounted on thin glass fibers with epoxy glue. Data sets were gathered using an Enraf-Nonius CAD4 automated four-circle diffractometer by standard procedures. Pertinent crystallographic data and data collection parameters are summarized in Table 2. Twenty-five reflections with $20° \le 2\theta \le 30°$ were located and centered. Their least-squares refinement resulted in monoclinic unit cells. The data sets were reduced by routine computational procedures. Absorption corrections based on azimuthal scans of reflections with χ angles near 90° were applied to the data sets. Intensities of three check reflections monitored at regular intervals remained invariant, indicating no sign of decay or decomposition of the crystals. The observed systematic absences indicated *C*2/*c* and *Cc* as the possible space groups. The choice of space group *C*2/*c* was proved to be correct from successful structure solutions and refinements for both compounds. The programs SHELXS-86 and SHELXL-93 were used for structure solutions and structure refinements, respectively.[10] The graphic programs[11] ATOMS and ORTEP were used to draw the structures.

For compound **1**, the positions of tungsten and two crystallographically distinct tellurium atoms, Te(1) and Te(2), were located by direct methods. Refinement of these positions and subsequent Fourier difference maps led to the location of the remaining atoms of the asymmetric unit, namely, one sodium atom and oxygen atoms O(1) to O(6). All the atoms were refined anisotropically, and the final Fourier difference map contained ghost peaks with ≤1.58 e/Å^3, very close to the heavy metal atoms, tungsten and tellurium.

The isostructural nature of compounds **1** and **2** was inferred from their similar X-ray powder diffraction patterns and lattice parameters. Therefore, compound **2** was modeled, starting with the refined positional parameters of **1**, and only tungsten was replaced by molybdenum. The final Fourier difference map, after successful anisotropic refinement, contained ghost peaks with ≤1.33 e/Å^3, very close to the heavy metal atoms, molybdenum and tellurium. The refined positional and equivalent isotropic thermal parameters for compounds **1** and **2** are given in Table 3. The bond lengths and selected bond angles are presented in Table 4.

Spectroscopic Data. The samples were ground with dry KBr and pressed into transparent disks. The infrared spectra were measured on these transparent disks from 400 to 4000 cm^{-1} for both compounds on a Bruker 17S, 66V FT-IR spectrometer.

Table 2. Crystallographic Data for $Na_2WTe_4O_{12}$ (**1**) and $Na_2MoTe_4O_{12}$ (**2**)

	1	**2**
empirical formula	$Na_2WTe_4O_{12}$	$Na_2MoTe_4O_{12}$
a (Å)	17.348(3)	17.341(4)
b (Å)	5.7755(10)	5.8262(11)
c (Å)	11.269(3)	11.268(2)
β (deg)	104.33(2)	104.38(2)
V (Å^3)	1094.0(4)	1102.7(4)
Z	4	4
fw	932.23	844.32
T (°C)	25	25
space group (No.)	*C*2/*c* (15)	*C*2/*c* (15)
λ(Mo Kα) (Å)	0.710 73	0.710 73
ρ_{calcd} (g/cm^3)	5.660	5.086
μ(Mo Kα) (mm^{-1})	21.157	11.702
R^a	0.0305	0.0288
R_w[b]	0.0891	0.0789

[a] $R = \sum||F_o| - |F_c||/\sum|F_o|$. [b] $R_w = [\sum w(|F_o|^2 - |F_c|^2)^2/\sum w(|F_o|^2)^2]^{1/2}$.

Table 3. Atomic Coordinates ($\times 10^4$) and Equivalent Isotropic Displacement Parameters (Å$^2 \times 10^3$) for $Na_2WTe_4O_{12}$ (**1**) and $Na_2MoTe_4O_{12}$ (**2**)

atom	*x*	*y*	*z*	U_{eq}[a]
		Compound **1**		
W	0	3404(1)	2500	7(1)
Te(1)	4045(1)	2833(1)	4035(1)	8(1)
Te(2)	3440(1)	1732(1)	651(1)	9(1)
O(1)	1095(4)	3991(15)	3402(7)	11(2)
O(2)	2423(4)	730(15)	747(8)	15(2)
O(3)	3370(5)	132(15)	4114(7)	14(2)
O(4)	3430(5)	3502(14)	2474(7)	13(2)
O(5)	4865(5)	1231(15)	3639(7)	14(2)
O(6)	260(5)	1471(15)	1441(8)	15(2)
Na	2119(3)	2289(9)	2677(5)	18(1)
		Compound **2**		
Mo	0	3401(2)	2500	10(1)
Te(1)	4040(1)	2760(1)	4052(1)	11(1)
Te(2)	3441(1)	1729(1)	677(1)	11(1)
O(1)	1098(3)	3975(9)	3389(5)	13(1)
O(2)	2432(3)	723(10)	735(5)	17(1)
O(3)	3377(3)	79(10)	4112(5)	17(1)
O(4)	3417(3)	3485(9)	2492(5)	14(1)
O(5)	4880(3)	1263(9)	3664(5)	14(1)
O(6)	247(3)	1555(10)	1450(5)	19(1)
Na	2104(2)	2275(6)	2653(3)	21(1)

[a] U_{eq} is defined as one-third of the trace of the orthogonalized $\mathbf{U}_{ij}$ tensor.

(9) Yvon, K.; Jeitschko, W.; Parthe, E. *J. Appl. Crystallogr.* **1977**, *10*, 73.

(10) (a) Sheldrick, G. M. *SHELXS-86 User Guide*; Crystallography Department, University of Gottingen: Gottingen, Germany, 1985. (b) Sheldrick, G. M. *SHELXL-93 User Guide*; Crystallography Department, University of Gottingen: Gottingen, Germany, 1993.

(11) (a) Dowty, E. *ATOMS*; Kingsport, TN, 1989. (b) Johnson, C. K. *ORTEP*; Oak Ridge National Laboratory: Oak Ridge, TN, 1970.

Table 4. Bond Lengths (Å) and Selected Bond Angles (deg) for $Na_2WTe_4O_{12}$ (**1**) and $Na_2MoTe_4O_{12}$ (**2**)

	1	2
M−O(6) × 2	1.773(8)	1.730(6)
M−O(1) × 2	1.950(8)	1.948(5)
M−O(5) × 2	2.125(8)	2.164(5)
Te(1)−O(5)	1.842(8)	1.840(5)
Te(1)−O(4)	1.859(8)	1.869(5)
Te(1)−O(3)	1.966(8)	1.951(6)
Te(2)−O(2)	1.885(8)	1.862(5)
Te(2)−O(1)	1.967(8)	1.975(5)
Te(2)−O(3)	2.018(8)	2.033(5)
Te(2)−O(4)	2.298(8)	2.296(5)
Te(2)−O(2)′	2.389(8)	2.414(6)
Na−O(1)	2.347(9)	2.330(6)
Na−O(4)	2.375(9)	2.376(6)
Na−O(4)	2.444(10)	2.433(6)
Na−O(2)	2.527(9)	2.534(6)
Na−O(3)	2.577(10)	2.548(7)
Na−O(2)	2.653(10)	2.694(7)
Na−O(3)	2.673(10)	2.722(7)
O(1)−M−O(1)′	160.0(5)	160.2(3)
O(1)−M−O(5) × 2	77.9(3)	77.6(2)
O(1)′−M−O(5) × 2	86.7(3)	87.1(2)
O(6)−M−O(1) × 2	94.8(4)	94.7(2)
O(6)′−M−O(1) × 2	97.8(4)	97.6(3)
O(5)−M−O(5)′	79.6(5)	79.1(3)
O(6)−M−O(5) × 2	167.2(4)	166.3(3)
O(6)′−M−O(5) × 2	89.6(4)	89.3(2)
O(6)−M−O(6)′	101.9(6)	103.1(4)
O(4)−Te(1)−O(3)	89.9(3)	90.3(2)
O(5)−Te(1)−O(3)	96.7(4)	97.9(2)
O(5)−Te(1)−O(4)	99.9(4)	101.0(2)
O(1)−Te(2)−O(2)	89.2(3)	89.1(2)
O(1)−Te(2)−O(2)′	163.3(3)	162.7(2)
O(1)−Te(2)−O(3)	88.0(3)	88.2(2)
O(1)−Te(2)−O(4)	88.1(3)	89.0(2)
O(2)−Te(2)−O(2)′	77.5(4)	77.0(2)
O(2)′−Te(2)−O(3)	82.3(3)	81.8(2)
O(2)−Te(2)−O(3)	91.5(3)	91.0(2)
O(2)−Te(2)−O(4)	82.6(3)	83.3(2)
O(2)′−Te(2)−O(4)	100.0(3)	99.5(2)
O(3)−Te(2)−O(4)	173.0(3)	173.7(2)
Te(1)−O(5)−M	137.7(4)	135.3(3)
Te(2)−O(1)−M	129.7(4)	128.9(3)
Te(1)−O(3)−Te(2)	123.5(4)	122.6(3)
Te(1)−O(4)−Te(2)	128.6(4)	127.1(3)
Te(2)−O(2)−Te(2)′	102.5(4)	103.0(2)

Results and Discussion

It is only the hydrothermal method that led to the isolation of these two new compounds, $Na_2WTe_4O_{12}$ (**1**) and $Na_2MoTe_4O_{12}$ (**2**), with hitherto unknown structure types, in the form of single crystals enabling the unambiguous identification of composition and structure determination. However, the successful solid state synthesis of these compounds in polycrystalline forms clearly shows that hydrothermal conditions are not necessary for their preparation. Thus, these compounds, stable even at temperatures of about 600 °C, are not metastable ones.

Crystal Structure. The isostructural compounds **1** and **2** have a three-dimensional anionic framework, $(MTe_4O_{12})^{2-}$, with different types of one-dimensional tunnels, one of them being occupied by Na^+ ions. The anionic framework can be conceived as being built by connecting, through MO_6 octahedra, two-dimensional Te_4O_{10} blocks formed from TeO_3 and TeO_5 polyhedra. Thus, three kinds of polyhedra, namely, $Te(1)O_3$ pyramids, $Te(2)O_5$ square pyramids, and MO_6 octahedra, constitute the anionic $(MTe_4O_{12})^{2-}$ framework.

Two $Te(2)O_5$ square pyramids share an edge to give rise to a Te_2O_8 moiety. Such moieties share four of their six corners with four $Te(1)O_3$ pyramids and each $Te(1)O_3$ pyramid, in turn, is corner-connected to two Te_2O_8 moieties as shown in Figure 1, resulting in two-dimensional blocks of composition Te_4O_{10}. It is to be noted that these two types of tellurite moieties, $Te(1)O_3$ and $Te(2)_2O_8$, are corner-connected in a spiral fashion and thereby the edges of these polyhedra form a spiral hexagonal tunnel. The word spiral is used in the present context to describe only the connectivity pattern of the edges of the polyhedra, which constitute the hexagonal tunnel. This tunnel is straight and parallel to the *b* axis. The two-dimensional Te_4O_{10} blocks are parallel to the *bc* plane.

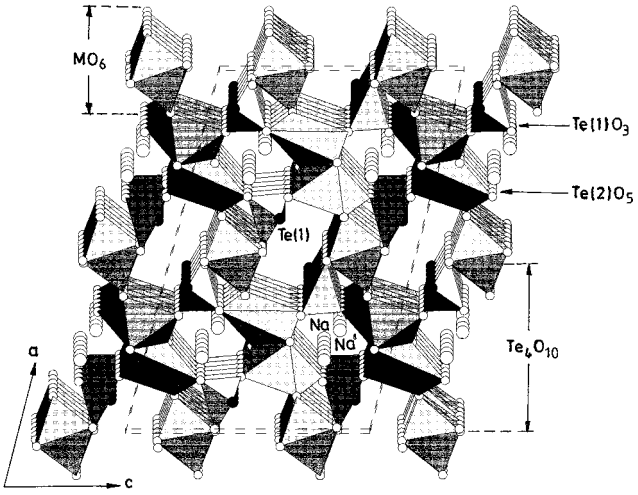

Figure 1. Unit cell diagram of $Na_2WTe_4O_{12}$ with the polyhedral representation of the $(WTe_4O_{12})^{2-}$ anionic framework. Filled spheres represent tellurium, and empty spheres of smaller and larger radii represent oxygen and sodium atoms, respectively. All spheres are of arbitrary radii.

Each MO_6 octahedron, with two cis corners unshared, is corner-connected to two $Te(1)O_3$ pyramids in a cis fashion and to two $Te(2)_2O_8$ moieties in a trans fashion and thus links two adjacent Te_4O_{10} blocks, resulting in the three-dimensional $(MTe_4O_{12})^{2-}$ anionic framework.. This anionic framework as shown in the unit cell diagram (Figure 1), contains triangular tunnels and pseudorectangular tunnels, both parallel to the *b* axis. The sides of these two tunnels are formed from all three types of polyhedra. Sodium ions are present in the spiral hexagonal tunnels. A different type of tunnel, of irregular shape, along the *c* axis and *C* centers, intersecting these three tunnels is also present (Figure 2).

All the atoms of the asymmetric unit represent only half of the formula unit, $Na_2MTe_4O_{12}$. Te(2) and the four oxygen atoms O(1) to O(4) account for half of Te_2O_8 moiety which sits on a crystallographic inversion center, and the halves are thus related by inversion symmetry. This moiety, as shown in Figure 3, has two TeO_5 square pyramids sharing an edge that involves the apical oxygen atoms, O(2) and O(2)′. O(2) forms an apical bond with one Te(2) and a basal bond with inversion-related Te(2)′. The Te−O bonds in this TeO_5 polyhedron range from 1.862 to 2.414 Å. The apical bond is shorter than the basal bonds, as reported for other TeO_5 square pydramids of $K_2Te_4O_{12}$[12] and $BaTe_2O_6$.[13] The O(2)−Te(2)-O(2)′ angle is about 77°, considerably smaller than the other O_{apical}−Te−O_{basal} angles of approximately 83−91° (Table 4). The tellurium atom lies about 0.19 Å below the basal plane of the square pyramid. All these data, when compared with those reported[12,13] for TeO_5 square

(12) Daniel, P. F.; Moret, J.; Maurin, M.; Philippot, E. *Acta Crystallogr.* **1978**, *B34*, 1782.

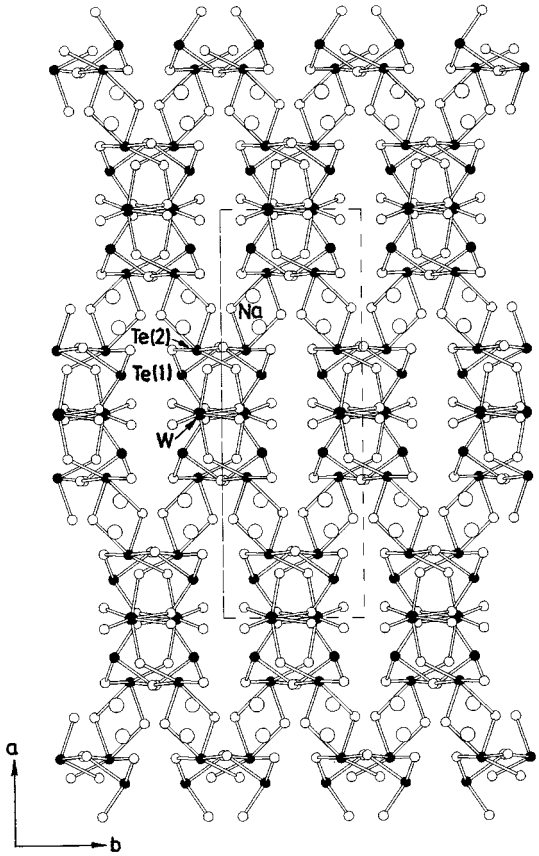

Figure 2. Unit cell diagram of $Na_2WTe_4O_{12}$ viewed perpendicular to the *ab* plane. Empty spheres of smaller radius represent oxygen atoms O(1)−O(6). All spheres are of arbitrary radii.

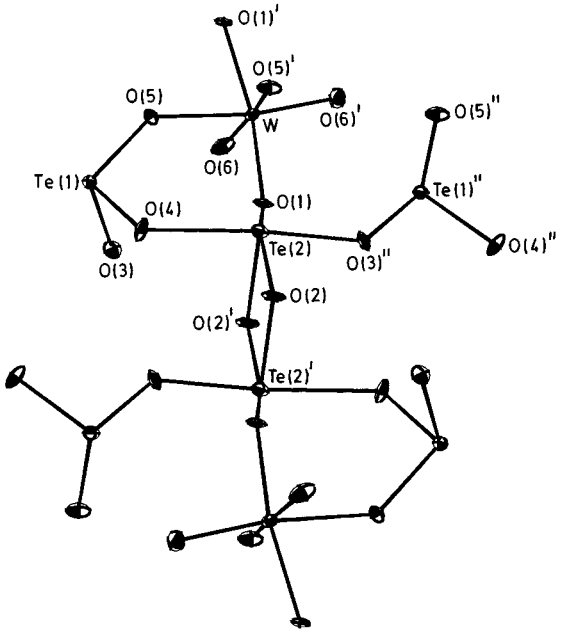

Figure 3. ORTEP plot showing the connectivity of the WO_6, Te(1)-O_3, and $Te(2)_2O_8$ moieties of $Na_2WTe_4O_{12}$, analog with the atom-labeling scheme (50% thermal ellipsoids).

pyramids, indicate the distortion of TeO_5 square pyramids in the title compounds.

Te(1) is pyramidally coordinated to three oxygen atoms, O(3), O(4), and O(5) (Figure 3), with Te−O bond lengths of 1.84−1.97 Å. The nonuniform O−Te−O bond angles indicate that the TeO_3 moiety is somewhat distorted. When compared with

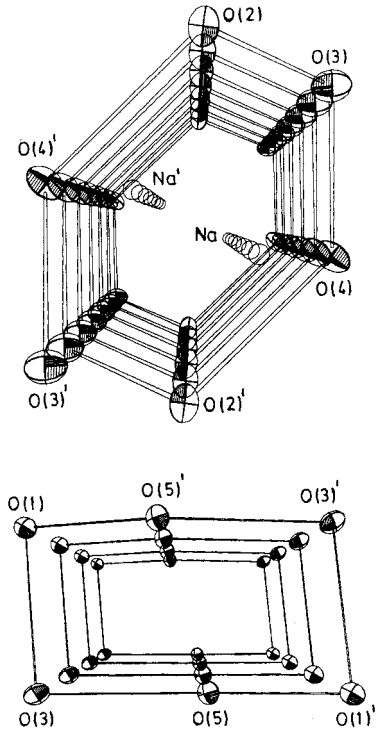

Figure 4. ORTEP plots of the oxygen atoms constituting the "hexagonal" tunnel (top) and "rectangular" tunnel (bottom) in $Na_2WTe_4O_{12}$, viewed approximately along the tunnel axis (50% thermal ellipsoids).

those of TeO_3 moieties of layered and zero-dimensional tellurites reported[6] by us, the O−Te−O angles are smaller, while the average Te−O bond lengths are similar. This $Te(1)O_3$ pyramid is corner-connected in a spiral fashion to the $Te(2)_2O_8$ moiety through O(3) and O(4) oxygen atoms. It is noteworthy that O(3)−Te(1)−O(4) is about 90°, considerably smaller than the other two bond angles of about 100° (Table 4).

The three oxygen atoms O(2) to O(4) form a spiral, leading to a pseudohexagonal tunnel (Figure 4), and the short, trans nonbonding O(2)···O(2)′, O(3)···O(3)′, and O(4)···O(4)′ distances in this tunnel are of the order of 4.87, 5.03, and 4.32 Å, respectively. The hexagonal tunnels observed in oxides such as hexagonal WO_3,[14] hexagonal tungsten bronze,[15] and $K_2W_4O_{13}$[16] have hexagonal windows perpendicular to the tunnel axis. These are distinctly different from the spiral pseudohexagonal tunnels of the title compounds wherein acyclic hexagonal windows are inclined to the tunnel axis. This is one of the interesting features of this compound. Similar spirals have been reported to be intertwined to give two strands of the double helix in $[(CH_3)_2NH_2]K_4V_{10}O_{10}(H_2O)_2(OH)_4(PO_4)_7 \cdot 4H_2O$.[17] Another feature of this compound is concerned with the coordination of Te^{4+}. There are only a few examples of tellurites[5,8,18,19] containing Te^{4+} in two different coordinations. The title compounds also contain Te^{4+} in two types of coordinaiton, but in a rare combination of pyramidal TeO_3 and square pyramidal TeO_5.

(13) Kocak, V. M.; Platte, C.; Tromel, M. *Acta Crystallogr.* **1979**, *B35*, 1439.
(14) Gerand, B.; Nowogrocki, G.; Guenot, J.; Figlarz, M. *J. Solid State Chem.* **1979**, 29, 429.
(15) Labbe, P. H.; Goreaud, M.; Raveau, B.; Monier, J. C. *Acta Crystallogr.* **1978**, *B34*, 1433.
(16) Seleborg, M. *J. Chem. Soc., Chem. Commun.* **1967**, 1126.
(17) Soghomonian, V.; Chen, Q.; Haushalter, R. C.; Zubieta, J.; O'Connor, C. J. *Science* **1993**, *259*, 1596.
(18) Lindqvist, O. *Acta Chem. Scand.* **1972**, *26*, 1423.
(19) Hanke, K.; Kupcik, V.; Lindqvist, O. *Acta Crystallogr.* **1973**, *B29*, 963.

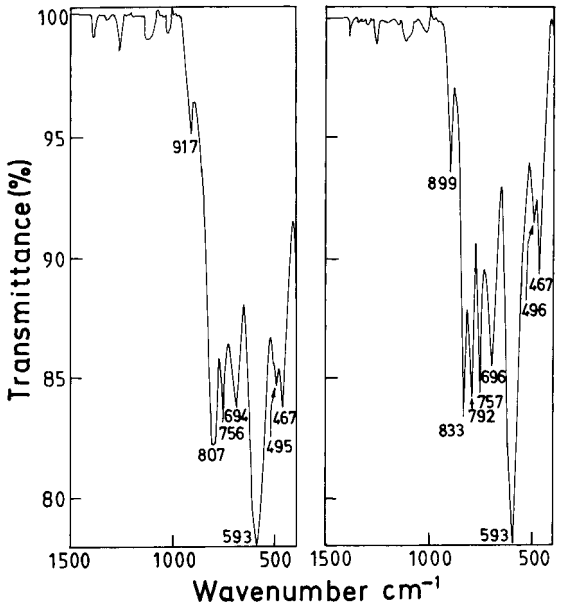

Figure 5. Infrared spectra of $Na_2WTe_4O_{12}$ (left) and $Na_2MoTe_4O_{12}$ (right).

The transition metal, molybdenum/tungsten, sits on a crystallographic 2-fold axis. It is octahedrally coordinated (Figure 3) to oxygen atoms O(1), O(5), and O(6) and their symmetry-related atoms. The two cis oxygen atoms O(6) and O(6)′ are exclusively bonded to the transition metal, and these two short M−O(6) bonds of 1.73−1.77 Å in length are trans to the long M−O(5) bonds. The O···O nonbonding edges vary from 2.57 to 2.84 Å, and the transition metal is displaced from the best centers[20] of the octahedra by 0.26 Å in compound **1** and 0.31 Å in compound **2**, toward the O(6)···O(6)′ nonbonding edge. The O−Mo−O bond angles deviate from the ideal value of 90° by as much as 13° (Table 4). These distortions of MO_6 octahedra are similar to those found in MoO_3[21] and $(NH_4)_6Mo_8Te_8O_{43}\cdot H_2O$.[8]

The nonbonding O(1)···O(3) edge of the $Te(2)_2O_8$ moiety forms the breadth and the two edges O(3)···O(5) of $Te(1)O_3$ and O(5)···O(1) of the MO_6 octahedron together form the length of the rectangular tunnel (Figure 4). The breadth, O(1)···O(3), is 2.8 Å, whereas the length is about 5.03 Å, less than the sum of nonbonding O(3)···O(5) and O(5)···O(1) distances, as a result of noncollinearity of O(3), O(5), and O(1). Thus the short O(1)···O(3) and long O(1)···O(3) nonbonding distances of 2.8 and 5.03 Å are the dimensions of the rectangular tunnel. The four corners, O(1), O(3), O(1)′, and O(3)′, are planar, and the four angles of this rectangle are nearly 90°. The lone pair of electrons of both Te(1) and Te(2) project into the void space of this rectangular tunnel. Our attempts to perform reductive intercalation of lithium into the tunnels of these compounds, using *n*-butyllithium in *n*-hexane as an intercalant, have not been successful. This could be due to the fact that the rectangular tunnels are not strictly empty but are occupied by stereoactive electron lone pairs of Te^{4+}. Similar rectangular tunnels formed from six edges of polyhedra are known in the compounds $Li_2Ti_3O_7$[22] and γ-MnO_2.[23]

Sodium ions residing in spiral hexagonal tunnels are coordinated to oxygen atom O(1) and two each of the spiral hexagonal tunnel oxygen atoms, O(2) to O(4). The NaO_7 polyhedron is of irregular shape, and the Na−O bonds range from 2.33 to 2.722 Å, with Na−O(1) being the shortest.

Spectroscopic Studies. The infrared spectra of compounds **1** and **2**, given in Figure 5, not only resemble closely those of other tellurites of molybdenum but also have similar features.[6−8] Here we assign only selected frequencies based on the limited literature available on the spectral characteristics of tellurites. The peaks around 917 and 807 cm^{-1} in the infrared spectrum of compound **1** and those around 899, 833, and 792 cm^{-1} in the infrared spectrum of compound **2** could be ascribed to M−O vibrations.[24−28] The peaks around 756, 694, and 593 cm^{-1} in the infrared spectra of compounds **1** and **2** could be due to one or more of the vibrations of M−O, Te−O, and M−O−Te, all of which fall in this range.[24−29]

Concluding Remarks

The present work involving the syntheses of $Na_2WTe_4O_{12}$ and $Na_2MoTe_4O_{12}$ is a good example of the isolation of new materials with novel structural features by hydrothermal techniques, in the form of single crystals, enabling unambiguous structural characterization. These two isostructural, tellurium-rich phases have an interesting three-dimensional structure with intersecting tunnels. The spiral nature of the connectivity pattern of pyramidal TeO_3 and square-pyramidal TeO_5 leading to hexagonal tunnels is a novel feature. Sodium ions reside in these novel spiral hexagonal tunnels.

Acknowledgment. We thank the Department of Science and Technology, Government of India, for financial support.

Supporting Information Available: X-ray crystallographic files, in CIF format, for $Na_2WTe_4O_{12}$ (**1**) and $Na_2MoTe_4O_{12}$ (**2**). This material is available free of charge via the Internet at http://pubs.acs.org.

IC990547I

(20) Zunic, T. B.; Makovicky, E. *Acta Crystallogr.* **1996**, *B52*, 78.
(21) Kihlborg, L. *Ark. Kemi* **1963**, *21*, 357.
(22) Morosin, B.; Mikkelsen, J. C. *Acta Crystallogr.* **1979**, *B35*, 798.
(23) Wolff, P. M. *Acta Crystallogr.* **1959**, *12*, 341.
(24) Griffith, W. P.; Wickins, T. D. *J. Chem. Soc. A* **1968**, 400.
(25) Griffith, W. P. *J. Chem. Soc. A* **1969**, 211.
(26) Rocchiccioli-Deltcheff, C.; Thouvenot, R.; Franck, R. *Spectrochim. Acta, Part A* **1975**, *32*, 587.
(27) Bart, J. C. J.; Cariati, F.; Sgamellotti, A. *Inorg. Chim. Acta* **1979**, *36*, 105.
(28) Dimitriev, Y.; Bart, J. C. J.; Dimitrov, V.; Arnaudov, M. *Z. Anorg. Allg. Chem.* **1981**, *479*, 229.
(29) Arnaudov, M.; Dimitrov, V.; Dimitriev, Y.; Markova, L. *Mater. Res. Bull.* **1982**, *17*, 1121.